

# Synthesis of Novel Alkyl Amide Functionalized Trifluoromethyl Substituted Furo/thieno Pyridine Derivatives: Their Anticancer Activity and CoMFA and CoMSIA Studies

Srinu Bhoomandla,<sup>a,b</sup> Shravan Kumar Gunda,<sup>c</sup> Srawanthi Kotoori,<sup>b</sup> and Phani Raja Kanuparth<sup>a\*</sup> 

<sup>a</sup>Department of Chemistry, Gitam University, Rudraram, Hyderabad, TS 502329, India

<sup>b</sup>Malla Reddy Institute of Technology and Science, Maisammaguda, Secunderabad, TS 500100, India

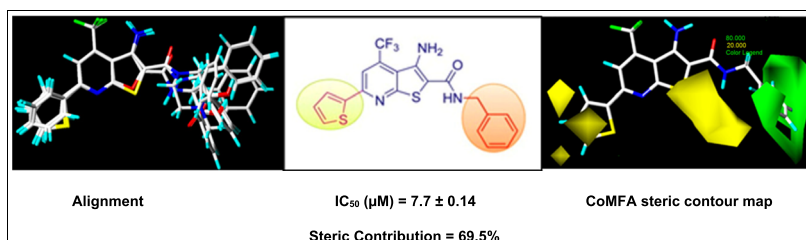
<sup>c</sup>Bioinformatics Division, PGRRCDE, Osmania University, Hyderabad, TS 500007, India

\*E-mail: phani.kpr@gmail.com

Received August 6, 2018

DOI 10.1002/jhet.3578

Published online 00 Month 2019 in Wiley Online Library (wileyonlinelibrary.com).



A series of novel alkyl amide functionalized trifluoromethyl substituted furo/thieno pyridine derivatives **4a–h**, **5a–d**, and **6a–h** were prepared starting from 2-oxo/thioxo-6-phenyl/thien-2-yl-4-(trifluoromethyl)-1,2-dihydropyridine-3-carbonitrile **1** on reaction with bromoethylacetate followed by reaction with different primary aliphatic amines, cyclic secondary amines, or L-amino acids under different set of conditions. All the synthesized compounds **4a–h**, **5a–d**, and **6a–h** were screened for anticancer activity against four cancer cell lines such as HeLa—cervical cancer (CCL-2), COLO205—colon cancer (CCL-222), HepG2—liver cancer (HB-8065), and MCF7—breast cancer (HTB-22). Compounds **4g** and **4h** are found to have promising anticancer activity at micromolar concentration. CoMFA and CoMSIA methods were applied to derive 3D-QSAR models for alkyl amide tagged furo/thieno pyridine derivatives as potential anticancer inhibitors. 3D-QSAR models provided a strong basis for future rational design of more active and selective HeLa, COLO205, HepG2, and MCF-7 cell line inhibitors.

*J. Heterocyclic Chem.*, **00**, 00 (2019).

## INTRODUCTION

During the past decade, cancer disease continued to be a worldwide killer [1]. The medicinal chemists have paid great attention to the development of novel lead molecule from natural source, and the demand is growing towards new therapies against cancer. Although chemotherapy is the mainstay for cancer treatment, the use of available chemotherapeutics is often limited due to undesirable side effects. Currently, a number of heterocyclic compounds are available commercially as anticancer agents. Fused pyridines are extensively used in neurology, particularly in the treatment of neurodegenerative disorders such as Parkinson's disease [2], antianxiety disorders [3], and depression [4]. Among all classes of biologically active heterocyclic compounds, the 5,6-fused ring systems such as furopyridines and thienopyridines attract in the development of new pharmaceutical agents and play an active role in the development of different medicinal agents [5–8]. These are structurally analogues to indoles and pyrrolopyridines and play a significant role in promoting activity [9,10]. Furopyridine and thienopyridine scaffolds are present in many bioactive molecules and acted against HIV [11–13], CNS disorders

[14], skin diseases [15], and hyperglycemia [16]. Trifluoromethylated drugs such as nilutamide, flutamide, hydroxyflutamide, and bicalutamide are nonsteroidal antiandrogens that are widely used for the treatment of metastatic prostate cancer [17,18]. Recently, it was found that the trifluoromethyl group [19–21] at a strategic position of an organic molecule dramatically alters the properties of molecule in terms of lipid solubility, oxidative thermal stability, permeability, and oral bioavailability.

Based on the importance of both the scaffolds furopyridine and thienopyridine, we assumed and synthesized novel alkyl amide functionalized trifluoromethyl substituted furo/thieno pyridine derivatives and submitted for anticancer activity against four cancer cell lines such as HeLa—cervical cancer, COLO205—colon cancer, HepG2—liver cancer, and MCF7—breast cancer. Compounds **4g** and **4h** are found to have promising anticancer activity at micromolar concentration.

The 2(1*H*) pyridine **1** was reacted with 2-bromoethyl acetate under basic conditions ( $K_2CO_3$ ) and obtained selectively 2-*O*-ethylacetoxo-3-cyano-4-trifluoro methyl-6-substituted pyridine derivatives **2**. Compounds **2** were

cyclized in DMF using potassium carbonate as base and obtained furo[2,3-*b*]pyridine derivatives **3**. The reaction sequence includes selective O-alkylation and then abstraction of proton by base from an active methylene followed cyclization onto nitrile carbon. This type of cyclization is also known as Thorpe–Ziegler cyclization. Compound **3** was further reacted with different primary aliphatic amines, cyclic secondary amines, or L-amino acids under various set of conditions and obtained *N*-alkyl acetamide pyrazolo[3,4-*b*]pyridine **4**, secondary amine ethanone tagged pyrazolo[3,4-*b*]pyridine **5**, and  $\alpha$ -amino acid functionalized pyrazolo[3,4-*b*]pyridine **6** derivatives, respectively. However, reaction of compound **3** with aromatic amines under different set of conditions such as (i) DMF,  $K_2CO_3$ , 110–120°C, 12–14 h, (ii) ethanol, Zn dust, sealed tube, 120°C, 10–12 h, and (iii)

DMSO,  $K_2CO_3$ , 150–160°C, 10–12 h could not give the product, and the starting material was recovered. It is attributed to the less basicity of aromatic amines compared with aliphatic amines. The synthetic sequence is drawn in Scheme 1, and products are tabulated in Table 1.

Compounds **4a–h**, **5a–d**, and **6a–h** were screened for *in vitro* against four cancer cell lines such as HeLa—cervical cancer (CCL-2), COLO205—colon cancer (CCL-222), HepG2—liver cancer (HB-8065), and MCF7—breast cancer (HTB-22) as A549 (lung cancer, CCL-185), MCF7 (breast cancer, HTB-22), DU145 (prostate cancer, HTB-81), and HeLa (cervical cancer, CCL-2) using MTT assay [22]. IC<sub>50</sub> values in micromolar concentration of the test compounds for 24 h on each cell line were calculated and presented in Table 2.

**Scheme 1.** Synthetic route of alkyl amide functionalized trifluoromethyl substituted furo/thieno pyridine derivatives **4a–h**, **5a–d**, and **6a–h**.

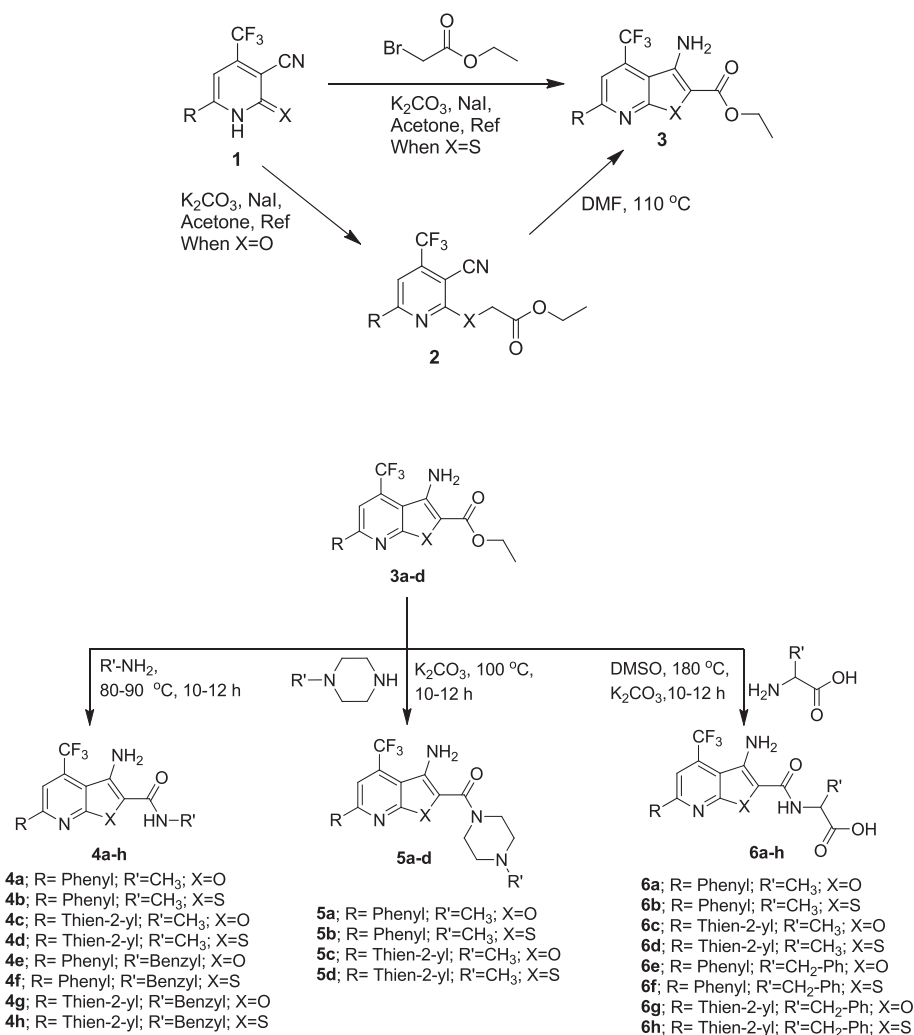


Table 1

Preparation of alkyl amide functionalized trifluoromethyl substituted furo/thieno pyridine derivatives **4a–h**, **5a–d**, and **6a–h**.

Entry	Compound	R	X	R'	Yield (%)
1.	<b>4a</b>	Phenyl	O	-CH <sub>3</sub>	90
2.	<b>4b</b>	Phenyl	S	-CH <sub>3</sub>	87
3.	<b>4c</b>	Thien-2-yl	O	-CH <sub>3</sub>	91
4.	<b>4d</b>	Thien-2-yl	S	-CH <sub>3</sub>	92
5.	<b>4e</b>	Phenyl	O	-CH <sub>2</sub> -C <sub>6</sub> H <sub>5</sub>	89
6.	<b>4f</b>	Phenyl	S	-CH <sub>2</sub> -C <sub>6</sub> H <sub>5</sub>	86
7.	<b>4g</b>	Thien-2-yl	O	-CH <sub>2</sub> -C <sub>6</sub> H <sub>5</sub>	89
8.	<b>4h</b>	Thien-2-yl	S	-CH <sub>2</sub> -C <sub>6</sub> H <sub>5</sub>	84
9.	<b>5a</b>	Phenyl	O	-CH <sub>3</sub>	82
10.	<b>5b</b>	Phenyl	S	-CH <sub>3</sub>	79
11.	<b>5c</b>	Thien-2-yl	O	-CH <sub>3</sub>	85
12.	<b>5d</b>	Thien-2-yl	S	-CH <sub>3</sub>	78
13.	<b>6a</b>	Phenyl	O	-CH <sub>3</sub>	82
14.	<b>6b</b>	Phenyl	S	-CH <sub>3</sub>	79
15.	<b>6c</b>	Thien-2-yl	O	-CH <sub>3</sub>	85
16.	<b>6d</b>	Thien-2-yl	S	-CH <sub>3</sub>	80
17.	<b>6e</b>	Phenyl	O	-CH <sub>2</sub> -C <sub>6</sub> H <sub>5</sub>	86
18.	<b>6f</b>	Phenyl	S	-CH <sub>2</sub> -C <sub>6</sub> H <sub>5</sub>	82
19.	<b>6g</b>	Thien-2-yl	O	-CH <sub>2</sub> -C <sub>6</sub> H <sub>5</sub>	88
20.	<b>6h</b>	Thien-2-yl	S	-CH <sub>2</sub> -C <sub>6</sub> H <sub>5</sub>	80

All the compounds except **5a** and **5b** showed activity against four cancer cell lines at micromolar concentration. Among all the compounds, **4g**, **4h**, **6d**, and **6g** showed promising activity, while the compounds **4c**, **4d**, **4f**, **6c**, and **6h** showed moderate activity. Compound **4h** was considered as the more potent towards all the cancer cell lines. The structure–activity relationship studies revealed that the thieno-2-yl group containing molecules showed more activity. In amide derivatives (**4a–h**), tagged aromatic amide derivatives are more potent compared with simple tagged aliphatic amide derivatives. Thienopyridine derivatives also showed promising activity, compared with furopyridine derivatives. Thienopyridine amide derivatives having thieno-2-yl group at 6th position and with tagged aromatic (benzyl) group showed promising cytotoxicity compared with phenyl group at 6th position of furopyridine ring. In conclusion, thieno-2-yl group and tagged aromatic (benzyl) groups are crucial for thienopyridine for promoting cytotoxic activity.

### QSAR INTRODUCTION

In general, the 3D-QSAR techniques are valuable methods of ligand-based drug design by correlating physicochemical properties from a set of related compounds to their known molecular property or molecular activity values. Validation of QSAR models plays the vital role in defining the applicability of the QSAR model for the prediction of designed molecules. QSAR model is mostly used to correlate properties, that

is, biological activities with chemical structures, and also used to predict the biological activity of nonsynthesized compounds; they are structurally related to training sets [23]. The present investigation reports the first application of 3D-QSAR to study of alkyl amide tagged furo/thieno pyridine derivatives as potent anticancer inhibitors. We studied 16 compounds for HeLa and COLO205 cell line inhibitors as anticancer agents using CoMFA (comparative molecular field analysis) [24] and CoMSIA (comparative molecular similarity indices analysis) [25]. Models obtained from 3D-QSAR studies provide a strong basis for future rational design of more active and selective HeLa and COLO205 cell line inhibitors.

### MATERIALS AND METHODS

**Data set.** In the present study, alkyl amide tagged furo/thieno pyridine derivatives as HeLa and COLO205 cell line inhibitors were selected for 3D-QSAR, and their biological data are presented in Table 1. The IC<sub>50</sub> values of alkyl amide tagged furo/thieno pyridine derivatives were often converted to their negative logarithm (pIC<sub>50</sub>) values. The pIC<sub>50</sub> values of these compounds range from 4.20 to 5.07 for HeLa cell lines and 4.28 to 5.11 for COLO205 cell lines, providing a wide range and homogenous data set for 3D-QSAR study. The data set was validated by external test set by taking **5** and **3** compounds that were selected randomly for HeLa and COLO205 targets, respectively. Remaining compounds were taken as the training set.

**Table 2**  
*In vitro* cytotoxicity of compounds **4a–h**, **5a–d**, and **6a–h**.

Compound	IC <sub>50</sub> values (in $\mu\text{M}$ )			
	HeLa	COLO205	HepG2	MCF7
<b>4a</b>	21.2 $\pm$ 0.18	32.5 $\pm$ 0.33	12.2 $\pm$ 0.51	—
<b>4b</b>	25.2 $\pm$ 0.22	31.3 $\pm$ 0.43	43.2 $\pm$ 0.11	45.2 $\pm$ 0.35
<b>4c</b>	17.5 $\pm$ 0.12	24.6 $\pm$ 0.21	21.4 $\pm$ 0.36	35.5 $\pm$ 0.25
<b>4d</b>	17.2 $\pm$ 0.23	16.1 $\pm$ 0.12	29.2 $\pm$ 0.38	31.5 $\pm$ 0.22
<b>4e</b>	21.1 $\pm$ 0.21	31.5 $\pm$ 0.34	119.2 $\pm$ 0.41	—
<b>4f</b>	24.2 $\pm$ 0.12	30.6 $\pm$ 0.29	32.6 $\pm$ 0.51	43.3 $\pm$ 0.32
<b>4g</b>	10.2 $\pm$ 0.12	11.7 $\pm$ 0.28	14.1 $\pm$ 0.20	12.8 $\pm$ 0.22
<b>4h</b>	8.5 $\pm$ 0.23	7.7 $\pm$ 0.14	11.5 $\pm$ 0.31	16.8 $\pm$ 0
<b>5a</b>	—	—	—	—
<b>5b</b>	—	—	—	—
<b>5c</b>	63.2 $\pm$ 0.52	—	—	—
<b>5d</b>	45.3 $\pm$ 0.22	38.9 $\pm$ 0.31	50.8 $\pm$ 0.33	41.7 $\pm$ 0.52
<b>6a</b>	50.2 $\pm$ 0.42	42.5 $\pm$ 0.36	49.8 $\pm$ 0.23	62.7 $\pm$ 0.38
<b>6b</b>	—	—	—	127.3 $\pm$ 0.32
<b>6c</b>	38.5 $\pm$ 0.18	18.9 $\pm$ 0.18	44.8 $\pm$ 0.42	31.5 $\pm$ 0.42
<b>6d</b>	19.2 $\pm$ 0.24	25.7 $\pm$ 0.24	12.8 $\pm$ 0.43	14.1 $\pm$ 0.18
<b>6e</b>	—	—	—	—
<b>6f</b>	44.6 $\pm$ 0.18	52.5 $\pm$ 0.21	66.2 $\pm$ 0.41	48.5 $\pm$ 0.22
<b>6g</b>	14.2 $\pm$ 0.14	15.8 $\pm$ 0.44	18.4 $\pm$ 0.24	21.2 $\pm$ 0.48
<b>6h</b>	24.5 $\pm$ 0.11	32.6 $\pm$ 0.25	44.1 $\pm$ 0.21	38.4 $\pm$ 0.42
<b>5-Fluorouracil</b> (standard control)	1.8 $\pm$ 0.09	1.9 $\pm$ 0.11	1.7 $\pm$ 0.08	1.8 $\pm$ 0.07

“—” indicates IC<sub>50</sub> value >127.3  $\mu\text{g}/\text{mL}$ . Cell lines used are as follows: HeLa—cervical cancer (CCL-2), COLO205—colon cancer (CCL-222), HepG2—liver cancer (HB-8065), and MCF7—breast cancer (HTB-22).

**Structure building and minimization.** All structures of alkyl amide tagged furo/thieno pyridine derivatives were sketched in SYBYL 6.7, a molecular modeling package, and energy minimization was performed to each and every alkyl amide tagged furo/thieno pyridine derivative using Tripos force field with distance-dependent dielectric function and Powell conjugate gradient algorithm with a convergence criterion of 0.005 kcal/mol; all the molecules were minimized by adding Gasteiger–Huckel charges [26].

**Molecular alignment.** In general, a geometric similarity should exist between the modeled structures and that of the bioactive conformation for 3D QSAR [27]. The spatial alignment of compounds under study is thus one of the most sensitive and determining factors in obtaining a reliable model. Molecular alignment plays a crucial role in CoMFA and CoMSIA studies [28]. The results of CoMFA and CoMSIA are extremely sensitive to a number of factors like alignment rules, orientation of the compounds that are aligned, probe atom type, and lattice shifting step size [29]. The accuracy of CoMFA and CoMSIA model prediction and contour analysis depends on structural alignment of molecules, and thus, we applied alignment to align all the molecules used in the current study. The molecular alignment was performed by using the SYBYL database align option. This option uses alignment of structures through pair-wise atom superpositioning that places all structures in the database

in the same frame of reference as the template compound. The most common part C-(4-trifluoromethyl-pyridin-3-yl)-methylamine of the most active compound **4h** was used for HeLa and COLO205 cell lines that were used as templates, and the remaining molecules were aligned to it through using the basic. The aligned molecules are shown in Figure 1.

**3D-QSAR studies.** For better comprehension of steric, electrostatic, hydrophobic, hydrogen-bond donor, and hydrogen-bond acceptor field contributions for the set of molecules, and to build predictive three-dimensional quantitative structure–activity relationship models, both CoMFA and CoMSIA studies were performed on the

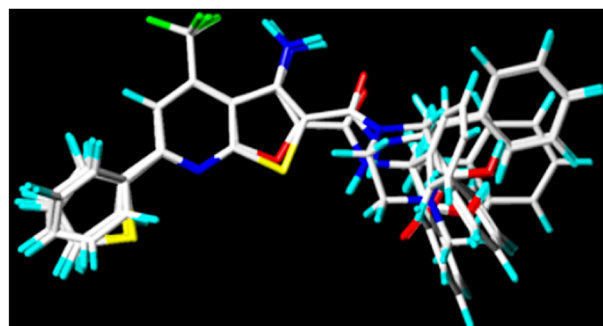


**Figure 1.** Alignment of all the compounds for HeLa cell line inhibitors and COLO205 cell line inhibitors. [Color figure can be viewed at [wileyonlinelibrary.com](http://wileyonlinelibrary.com)]

basis of molecular alignment as described earlier. CoMFA calculates steric and electrostatic properties, whereas CoMSIA calculates hydrophobic, donor, and acceptor properties along with steric and electrostatic properties. CoMFA and CoMSIA properties are calculated with respect to Lennard–Jones and Columbic potentials.

**CoMFA studies.** Steric and electrostatic properties were calculated using Tripos force field engine, and the aligned molecules were placed in a 3D grid box so that the entire set was included. CoMFA descriptors were generated using sp<sup>3</sup> probe atom carrying +1 charge to generate steric and electrostatic fields; 30-kcal/mol cut-off was used for the analysis, and standard options were used for the calculation of regression analysis. Partial least square was performed by selecting leave-one-out using 5 as the number of components, and the column filtering was set as 2.0 kcal/mol.

**CoMSIA studies.** CoMSIA analysis was performed with the QSAR option in SYBYL. Five different properties were used in CoMSIA studies, which are steric, electrostatic, hydrophobic, donor, and acceptor, based on which similarity indices between a probe atom and compound were calculated. The probe atom with 1-Å radius, +1 charge, and +1 for hydrophobicity was set at the intersections of the lattice.

## RESULTS AND DISCUSSION

**CoMFA and CoMSIA.** CoMFA and CoMSIA methods were applied to derive 3D-QSAR models for alkyl amide tagged furo/thieno pyridine derivatives as potential

anticancer inhibitors. The statistical results of CoMFA and CoMSIA analyses are summarized in Table 3. The best predictions were obtained with CoMFA standard model involving cross-validated coefficient ( $q^2$ ) = 0.791 for HeLa and 0.772 for COLO205 and correlation coefficient ( $r^2$ ) = 0.996 and 0.989 for HeLa and COLO205, respectively. Standard error of estimate = 0.046 for HeLa and 0.035 for COLO205. Cross-validation = 0.796 and 0.770 for HeLa and COLO205, respectively, with number of components as 5 and column filtering as 2.0 kcal/mol. In CoMSIA, the standard model predictions obtained are  $q^2$  = 0.779 for HeLa and 0.722 for COLO205,  $r^2$  = 0.991 for HeLa and 0.984 for COLO205, standard error of estimate = 0.061 and 0.045 for HeLa and COLO205, respectively, and cross-validation = 0.793 and 0.733 for HeLa and COLO205, respectively, with number of components as 6 and column filtering as 1.0 kcal/mol. Both the targets show better predictive ability for these compounds. Bootstrapping method is used to evaluate the robustness and the statistical confidence of the QSAR model. It involves simulating a large number of data sets that are of the same size as original and are produced by randomly selecting samples from the original set. Biological activities and predicted and residual values of both training set and test set CoMFA and CoMSIA are shown in Table 3.

Table 3 shows the results of relative contributions for CoMFA and CoMSIA methods. For CoMFA, steric contributions are 51.5% and 69.5% for HeLa and COLO205, respectively, and 48.5% and 30.5% field contribution was observed for electrostatic respectively for HeLa and COLO205 cell lines, whereas for CoMSIA,

**Table 3**

The statistical results of CoMFA and CoMSIA analysis.

	HeLa				COLO205			
	CoMFA	CoMSIA			CoMFA	CoMSIA		
$q^2$	0.791	0.799			0.772	0.722		
$r^2$	0.996	0.991			0.989	0.984		
SEE	0.046	0.061			0.035	0.045		
<i>F</i> -value	95.713	43.676			82.062	37.099		
CV	0.796	0.793			0.770	0.733		
<i>N</i>	5	6			5	6		
Bootstrap								
	Mean	SD	Mean	SD	Mean	SD	Mean	SD
SEE	0.016	0.013	0.011	0.010	0.025	0.021	0.015	0.020
$r^2$	0.997	0.001	0.999	0.001	0.993	0.006	0.998	0.003
Field contribution (%)								
Steric	51.5	18.5			69.5	22.1		
Electrostatic	48.5	21.4			30.5	18.6		
Hydrophobic	—	30.0			—	34.3		
Donor	—	11.1			—	8.70		
Acceptor	—	19.1			—	16.3		

CV, cross-validation; SEE, standard error of estimate.

the observed contributions for steric, electrostatic, hydrophobic, donor, and acceptor properties are given in Table 2. Electrostatic property is the main contributor in CoMSIA analysis.

Tables 4–7 indicate experimental and cross-validated/predicted biological affinities and residuals obtained by the CoMFA and CoMSIA for alkyl amide tagged furo/thieno pyridine derivatives as HeLa and COLO205 cell line inhibitors. For HeLa cell line, CoMFA results show a higher predictive ability for alkyl amide tagged furo/thieno pyridine derivatives against anticancer on comparison with CoMSIA results. For COLO205 cell line, CoMSIA results show a higher predictive ability for

alkyl amide tagged furo/thieno pyridine derivatives against anticancer on comparison with CoMFA results (Tables 4–7).

**Contour analysis. CoMFA and CoMSIA steric contour plots.** For HeLa, the CoMFA model was used to generate the three-dimensional contour maps to represent the quantitative structure activity result. A single large green isopleth is present above amide tagged benzyl ring; it indicates that the position contains more steric hindrance. The compound shows four yellow contours at thieno pyridine ring and three contours at thiophene ring, which indicates that steric hindrance is less. In CoMSIA, a very large green contour present amide tagged benzyl ring,

**Table 4**

Test set: Experimental and cross-validated/predicted biological affinities and residuals obtained by the CoMFA and CoMSIA for alkyl amide tagged furo/thieno pyridine derivatives as HeLa cell line inhibitors.

Compound	pIC <sub>50</sub>	CoMFA		CoMSIA	
		Predicted	Residual	Predicted	Residual
<b>4b</b>	4.60	4.80	-0.20	4.77	-0.17
<b>4e</b>	4.67	5.03	-0.36	5.04	-0.37
<b>4f</b>	4.62	4.86	-0.24	4.87	-0.25
<b>6d</b>	4.72	4.04	0.68	4.37	0.35
<b>6g</b>	4.85	4.51	0.34	4.45	0.40

**Table 5**

Training set: Experimental and cross-validated/predicted biological affinities and residuals obtained by the CoMFA and CoMSIA for alkyl amide tagged furo/thieno pyridine derivatives as HeLa cell line inhibitors.

Compound	pIC <sub>50</sub>	CoMFA		CoMSIA	
		Predicted	Residual	Predicted	Residual
<b>4a</b>	4.67	4.63	0.04	4.61	0.06
<b>4c</b>	4.76	4.72	0.04	4.75	0.01
<b>4d</b>	4.76	4.57	0.19	4.72	0.04
<b>4g</b>	4.99	4.72	0.27	4.88	0.11
<b>4h</b>	5.07	4.73	0.34	4.85	0.22
<b>6a</b>	4.30	4.25	0.05	4.19	0.11
<b>6c</b>	4.41	4.48	-0.07	4.52	-0.11
<b>6f</b>	4.35	4.53	-0.18	4.52	-0.17
<b>6h</b>	4.61	4.47	0.14	4.49	0.12

**Table 6**

Test set: Experimental and cross-validated/predicted biological affinities and residuals obtained by the CoMFA and CoMSIA for alkyl amide tagged furo/thieno pyridine derivatives as COLO205 cell line inhibitors.

Compound	pIC <sub>50</sub>	CoMFA		CoMSIA	
		Predicted	Residual	Predicted	Residual
<b>4f</b>	4.51	4.81	-0.30	4.84	-0.33
<b>5d</b>	4.41	4.91	-0.50	4.78	-0.37
<b>6d</b>	4.59	4.57	0.02	4.58	0.01

Table 7

Training set: Experimental and cross-validated/predicted biological affinities and residuals obtained by the CoMFA and CoMSIA for alkyl amide tagged furo/thieno pyridine derivatives as COLO205 cell line inhibitors.

Compound	pIC <sub>50</sub>	CoMFA		CoMSIA	
		Predicted	Residual	Predicted	Residual
4a	4.49	4.45	0.04	4.36	0.13
4b	4.5	4.63	-0.13	4.65	-0.15
4c	4.61	4.68	-0.07	4.74	-0.13
4d	4.79	4.69	0.10	4.66	0.13
4e	4.50	4.63	-0.13	4.63	-0.13
4g	4.93	4.72	0.21	4.78	0.15
4h	5.11	4.79	0.32	4.86	0.25
6a	4.37	4.51	-0.14	4.48	-0.11
6c	4.72	4.59	0.13	4.61	0.11
6f	4.28	4.24	0.04	4.21	0.07
6g	4.8	4.67	0.13	4.65	0.15
6h	4.49	4.58	-0.09	4.58	-0.09

which increases the steric hindrance, and a large yellow contour below the amide ring. Adding bulk groups at this ring decreases the biological activity.

In CoMFA, the most active compound showed two green contours, a large and green contour. A large polyhedron is present above amide tagged benzyl ring and a small polyhedron below the thiophene ring, indicating steric favorable region where biological activity increases by adding bulky groups. One big and one small yellow contours are present, covering thiophene ring where bulky groups decrease the activity of the compound. In CoMSIA, the most active compound shows that a large green contour is present above amide

tagged benzyl ring, where activity increases, and two large yellow contours are present above amide tagged benzyl ring, covering thiophene ring, which decreases the activity by adding bulk groups. The most active compound shows that yellow and green contours are present, which are shown in Figure 2.

**CoMFA electrostatics contours plots.** For HeLa, the electrostatic contours maps of CoMFA and CoMSIA are shown in blue and red colors. In both CoMFA and CoMSIA, medium-sized blue contours are present near amide tagged benzyl ring, indicating that addition of positive charge groups may increase the biological activity of a compound. The blue contours are in

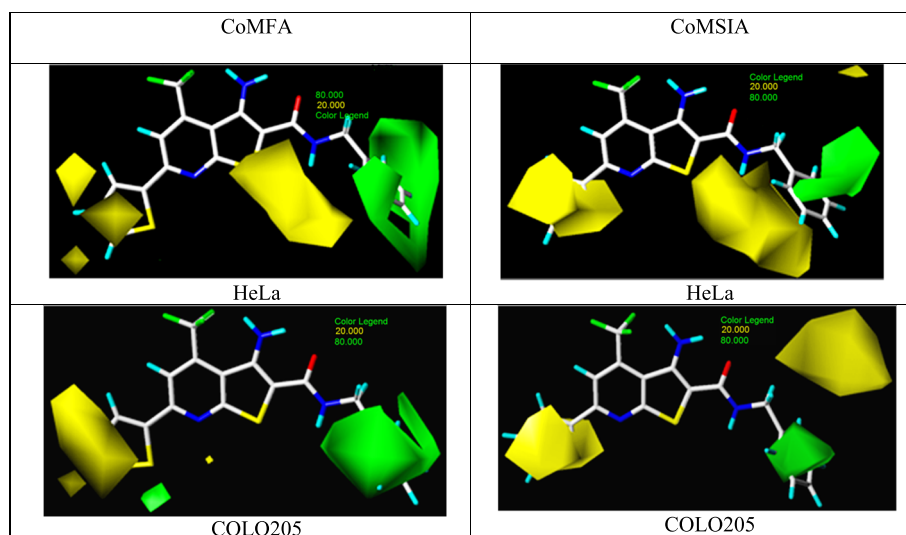


**Figure 2.** CoMFA and CoMSIA contour maps of the most active compound. Sterically favored areas are shown in green color (contribution level of 80%). Sterically unfavored areas are shown in yellow color (contribution level of 20%). [Color figure can be viewed at [wileyonlinelibrary.com](http://wileyonlinelibrary.com)]

favorable region and red contours in disfavored region. A very small-sized red contour and a medium-sized red contour are present above amide tagged benzyl ring; at this position, electron density is estimated to increase the biological activity. Adding electro-negative groups may enhance the activity. For COLO205, a small blue-colored contour is present near amide tagged benzyl ring, and medium-sized red-colored contours are present above amide tagged benzyl ring, shown in Figure 3. In CoMSIA, blue contour is present above thiophene ring, where addition of negative groups enhances the biological activity.

**CoMSIA hydrophobic contour analysis.** CoMSIA hydrophobic contour maps are shown in yellow and white colors. For HeLa, two medium-sized yellow contours present amide tagged benzyl ring. For COLO205, a large yellow contour is present by covering the amide tagged benzyl ring; this indicates favorable

hydrophobic substitution, shown in Figure 4. For both HeLa and COLO205, a large white contour is present around thiophene, indicating disfavored conformation for hydrophobic substitution.

**CoMSIA hydrogen-bond donor contour analysis.** The graphical representation of the field contributions of the hydrogen-bond donor is shown in Figure 5. Donor contour maps are shown in cyan and purple colors. Cyan contour maps explain the position of hydrogen-bond donor groups, which increases biological activity, while purple contours are biologically unflavored, shown in Figure 5. For HeLa, a large cyan-colored contour is present around amide tagged benzyl ring, and in COLO205, the most active compound shows a small cyan isopleth above amide tagged benzyl ring, which enhance the biological activity, and two medium-sized purple isopleths are present around amide tagged benzyl ring, which reduce the biological activity.

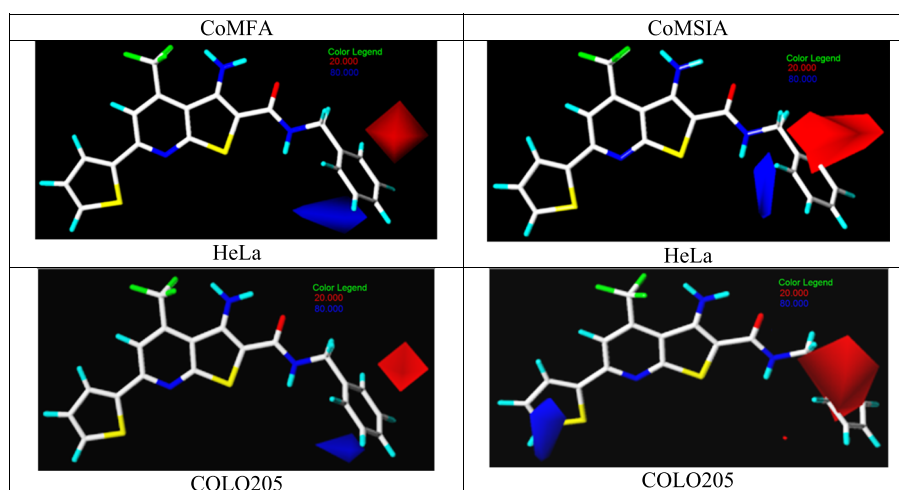


**Figure 3.** CoMFA and CoMSIA electrostatic contour maps of the most active compound. Positive potential favored areas are shown in blue color (contribution level of 80%). Positive potential unfavored areas are shown in red color (contribution level of 20%). [Color figure can be viewed at [wileyonlinelibrary.com](http://wileyonlinelibrary.com)]

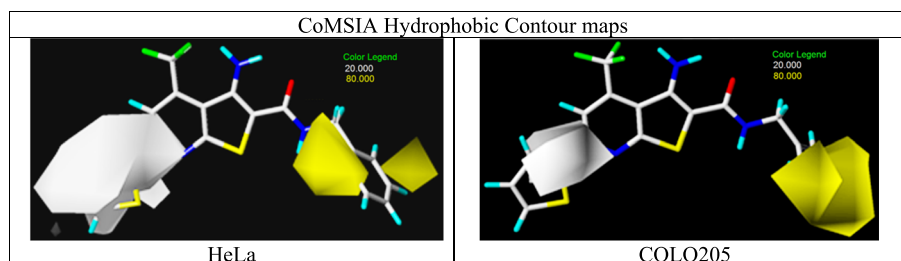


**Figure 4.** Hydrophobic contour maps are shown in yellow and white areas, indicating where hydrophobic amino acid residues will increase or decrease the affinity, respectively. [Color figure can be viewed at [wileyonlinelibrary.com](http://wileyonlinelibrary.com)]

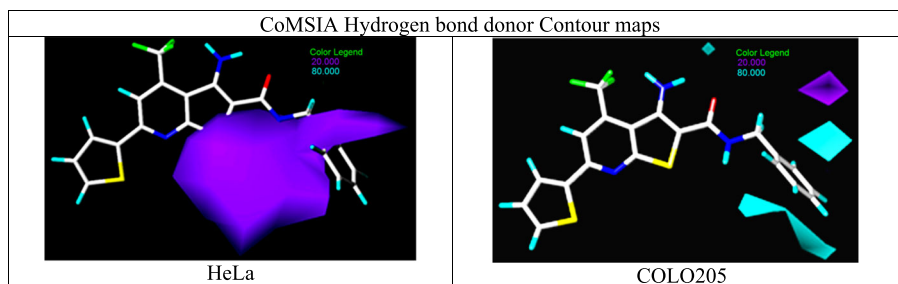


**Figure 5.** Hydrogen-bond donor contours are shown in cyan and purple areas, indicating where hydrogen-bond donor groups on the ligand will increase or decrease the affinity. [Color figure can be viewed at [wileyonlinelibrary.com](http://wileyonlinelibrary.com)]

#### COMSIA hydrogen-bond acceptor contour analysis.

Hydrogen-bond acceptor contours are represented in magenta and red colors. Magenta color indicates favorable region, and red color indicates unfavorable region of biological activity. In HeLa, the most active compound shows two large magenta isopleths, one magenta polyhedron covering amide tagged benzyl ring and one above amide tagged benzyl ring, whereas in COLO205, the most active compound shows that a medium-sized magenta and a large red contour and a small red contour are present, which are shown in Figure 6.

**General procedure.** Ethyl 3-amino-6-(phenyl/thiophen-2-yl)-4-(trifluoromethyl) furo/thieno[2,3-*b*]pyridine-2-carboxylate **3** (0.01 mol) reacted with different primary aliphatic amines (0.015 mol) at 80–90°C for 10–12 h; after completion of the reaction, reaction mixture was poured into crushed ice, and solid was formed. This solid was filtered and dried to afford the solid product **4**.

**3-Amino-N-methyl-6-phenyl-4-(trifluoromethyl)furo[2,3-*b*]pyridine-2-carboxamide (4a).** Pale yellow solid; mp 185–187°C; IR (KBr,  $\text{cm}^{-1}$ ): 1660 (–CONH–);  $^1\text{H}$  NMR (DMSO- $d_6$ , 300 MHz):  $\delta$  ppm 2.68 (s, 3H, –N–CH<sub>3</sub>), 6.52 (br s, 2H, –NH<sub>2</sub>), 7.32 (br s, 1H, –CONH–), 7.48–7.56 (m, 3H, Ar–H), 7.78 (s, 1H, Py–H), 8.10–8.17 (m, 2H, Ar–H);  $^{13}\text{C}$  NMR (DMSO- $d_6$ , 75 MHz):  $\delta$  ppm 25.4, 119.3, 125.2, 125.5, 127.1, 128.1, 129.0, 130.6, 133.6,

134.9, 137.3, 139.9, 142.2, 160.9; MS (ESI):  $m/z$  [(M + H)<sup>+</sup>]: 336. HRMS  $m/z$  Calcd for C<sub>16</sub>H<sub>12</sub>F<sub>3</sub>N<sub>3</sub>O<sub>2</sub> [(M + H)<sup>+</sup>]: 336.0369. Found: 336.0371.

**3-Amino-N-methyl-6-phenyl-4-(trifluoromethyl)thieno[2,3-*b*]pyridine-2-carboxamide (4b).** Yellow solid; mp 171–173°C; IR (KBr,  $\text{cm}^{-1}$ ): 1662 (–CONH–);  $^1\text{H}$  NMR (DMSO- $d_6$ , 300 MHz):  $\delta$  ppm 2.74 (s, 3H, –N–CH<sub>3</sub>), 6.53 (br s, 2H, –NH<sub>2</sub>), 7.38 (br s, 1H, –CONH–), 7.43–7.52 (m, 3H, Ar–H), 7.79 (s, 1H, Py–H), 7.90–7.95 (m, 2H, Ar–H);  $^{13}\text{C}$  NMR (DMSO- $d_6$ , 75 MHz):  $\delta$  ppm 25.2, 123.1, 123.7, 125.3, 126.0, 128.0, 129.0, 129.8, 129.9, 131.3, 133.4, 133.8, 134.6, 162.3; MS (ESI):  $m/z$  [(M + H)<sup>+</sup>]: 352. HRMS  $m/z$  Calcd for C<sub>16</sub>H<sub>12</sub>F<sub>3</sub>N<sub>3</sub>OS [(M + H)<sup>+</sup>]: 352.0116. Found: 352.0118.

**3-Amino-N-methyl-6-(thiophen-2-yl)-4-(trifluoromethyl)furo[2,3-*b*]pyridine-2-carboxamide (4c).** Yellow solid; mp 161–162°C; IR (KBr,  $\text{cm}^{-1}$ ): 1664 (–CONH–);  $^1\text{H}$  NMR (DMSO- $d_6$ , 300 MHz):  $\delta$  ppm 2.73 (s, 3H, –N–CH<sub>3</sub>), 6.51 (br s, 2H, –NH<sub>2</sub>), 7.32 (br s, 1H, –CONH–), 7.51 (dd,  $J = 4.15$ , 1H, Ar–H), 7.75 (dd,  $J = 4.91$ , 1H, Ar–H), 7.98 (s, 1H, Py–H), 8.14 (dd,  $J = 3.77$ , 1H, Ar–H);  $^{13}\text{C}$  NMR (DMSO- $d_6$ , 75 MHz):  $\delta$  ppm 26.2, 122.0, 125.4, 125.8, 127.0, 128.1, 130.0, 132.0, 134.7, 137.4, 139.9, 142.1, 143.6, 160.5; MS (ESI):  $m/z$  [(M + H)<sup>+</sup>]: 342. HRMS  $m/z$

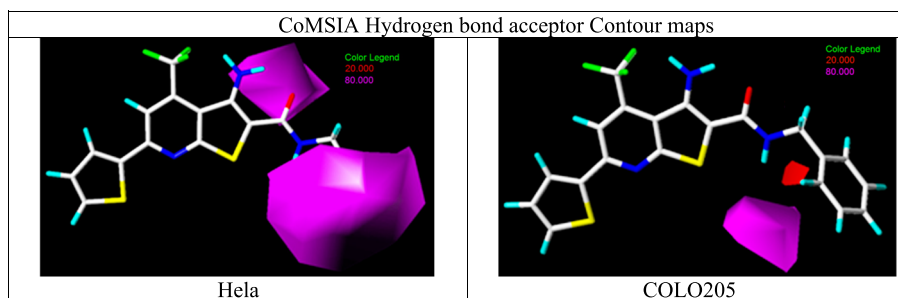


**Figure 6.** Magenta and red areas indicate where hydrogen-bond acceptor groups on the ligand will increase or decrease the affinity, respectively Alkyl amide tagged furo/thieno pyridine derivatives as HeLa cell line inhibitor. [Color figure can be viewed at [wileyonlinelibrary.com](http://wileyonlinelibrary.com)]

Calcd for  $C_{14}H_{10}F_3N_3O_2S$  [(M + H)<sup>+</sup>]: 342.0553. Found: 342.0551.

**3-Amino-N-methyl-6-(thiophen-2-yl)-4-(trifluoromethyl)thieno[2,3-b]pyridine-2-carboxamide (4d).** Yellow solid; mp 184–186°C; IR (KBr,  $cm^{-1}$ ): 1662 (–CONH–); <sup>1</sup>H NMR (DMSO-*d*<sub>6</sub>, 300 MHz): δ ppm 2.72 (s, 3H, –N–CH<sub>3</sub>), 6.52 (br s, 2H, –NH<sub>2</sub>), 7.33 (br s, 1H, –CONH–), 7.52 (dd, *J* = 4.72, 1H, Ar–H), 7.65 (dd, *J* = 4.73, 1H, Ar–H), 7.81 (s, 1H, Py–H), 8.84 (dd, *J* = 3.72, 1H, Ar–H); <sup>13</sup>C NMR (DMSO-*d*<sub>6</sub>, 75 MHz): δ ppm 25.4, 121.9, 123.5, 124.6, 125.7, 127.7, 128.3, 129.0, 130.2, 135.9, 137.9, 162.3; MS (ESI): *m/z* [(M + H)<sup>+</sup>]: 358. HRMS *m/z* Calcd for  $C_{14}H_{10}F_3N_3OS_2$  [(M + H)<sup>+</sup>]: 358.1012. Found: 358.1015.

**3-Amino-N-benzyl-6-phenyl-4-(trifluoromethyl)furo[2,3-b]pyridine-2-carboxamide (4e).** Pale yellow solid; mp 192–193°C; IR (KBr,  $cm^{-1}$ ): 1667 (–CONH–); <sup>1</sup>H NMR (DMSO-*d*<sub>6</sub>, 300 MHz): δ ppm 4.35 (d, 2H, *J* = 5.86, –CH<sub>2</sub>–N–), 6.53 (br s, 2H, –NH<sub>2</sub>), 7.32 (br s, 1H, –CONH–), 7.41–7.58 (m, 6H, Ar–H), 7.79 (s, 1H, Py–H), 8.10–8.18 (m, 4H, Ar–H); <sup>13</sup>C NMR (DMSO-*d*<sub>6</sub>, 75 MHz): δ ppm 46.0, 119.0, 120.1, 122.3, 122.6, 123.9, 124.8, 125.8, 127.9, 128.9, 130.8, 133.9, 134.3, 135.5, 137.4, 144.5, 145.1, 160.1; MS (ESI): *m/z* [(M + H)<sup>+</sup>]: 412. HRMS *m/z* Calcd for  $C_{22}H_{16}F_3N_3O_2$  [(M + H)<sup>+</sup>]: 412.0229. Found: 412.0231.

**3-Amino-N-benzyl-6-phenyl-4-(trifluoromethyl)thieno[2,3-b]pyridine-2-carboxamide (4f).** Dark yellow solid; mp 197–199°C; IR (KBr,  $cm^{-1}$ ): 1666 (–CONH–); <sup>1</sup>H NMR (DMSO-*d*<sub>6</sub>, 300 MHz): δ ppm 4.34 (d, 2H, *J* = 5.83, –CH<sub>2</sub>–N–), 6.51 (br s, 2H, –NH<sub>2</sub>), 7.35 (br s, 1H, –CONH–), 7.44–7.60 (m, 6H, Ar–H), 7.81 (s, 1H, Py–H), 8.12–8.19 (m, 4H, Ar–H); <sup>13</sup>C NMR (DMSO-*d*<sub>6</sub>, 75 MHz): δ ppm 46.1, 119.9, 120.8, 123.0, 123.4, 124.6, 125.6, 126.4, 127.9, 129.6, 131.4, 133.9, 134.2, 135.6, 137.3, 141.8, 147.9, 160.1; MS (ESI): *m/z* [(M + H)<sup>+</sup>]: 428. HRMS *m/z* Calcd for  $C_{22}H_{16}F_3N_3OS$  [(M + H)<sup>+</sup>]: 428.0105. Found: 428.0108.

**3-Amino-N-benzyl-6-(thiophen-2-yl)-4-(trifluoromethyl)furo[2,3-b]pyridine-2-carboxamide (4g).** Yellow solid; mp 151–152°C; IR (KBr,  $cm^{-1}$ ): 1661 (–CONH–); <sup>1</sup>H NMR (DMSO-*d*<sub>6</sub>, 300 MHz): δ ppm 4.34 (d, 2H, *J* = 5.85, –CH<sub>2</sub>–N–), 6.52 (br s, 2H, –NH<sub>2</sub>), 7.32 (br s, 1H, –CONH–), 7.43 (dd, *J* = 4.72, 1H, Ar–H), 7.49–7.57 (m, 3H, Ar–H), 7.64–7.71 (m, 2H, Ar–H), 7.78 (dd, *J* = 4.72, 1H, Ar–H), 7.82 (dd, *J* = 3.72, 1H, Ar–H), 8.24 (s, 1H, Py–H); <sup>13</sup>C NMR (DMSO-*d*<sub>6</sub>, 75 MHz): δ ppm 46.2, 118.0, 119.0, 121.1, 121.6, 122.7, 123.7, 124.5, 126.0, 127.7, 129.5, 132.0, 132.4, 133.7, 137.9, 139.9, 147.0, 160.3; MS (ESI): *m/z* [(M + H)<sup>+</sup>]: 418. HRMS *m/z* Calcd for  $C_{20}H_{14}F_3N_3O_2S$  [(M + H)<sup>+</sup>]: 418.0342. Found: 418.0343.

**3-Amino-N-benzyl-6-(thiophen-2-yl)-4-(trifluoromethyl)thieno[2,3-b]pyridine-2-carboxamide (4h).** Yellow solid; mp 165–166°C; IR (KBr,  $cm^{-1}$ ): 1665 (–CONH–); <sup>1</sup>H

NMR (DMSO-*d*<sub>6</sub>, 300 MHz): δ ppm 4.32 (d, 2H, *J* = 5.83, –CH<sub>2</sub>–N–), 6.51 (br s, 2H, –NH<sub>2</sub>), 7.32 (br s, 1H, –CONH–), 7.41 (dd, *J* = 4.71, 1H, Ar–H), 7.48–7.58 (m, 3H, Ar–H), 7.62–7.68 (m, 2H, Ar–H), 7.86 (dd, *J* = 4.74, 1H, Ar–H), 7.96 (dd, *J* = 3.75, 1H, Ar–H), 8.09 (s, 1H, Py–H); <sup>13</sup>C NMR (DMSO-*d*<sub>6</sub>, 75 MHz): δ ppm 46.0, 119.7, 120.6, 122.0, 123.9, 125.4, 126.0, 127.7, 128.9, 129.8, 130.7, 132.2, 133.8, 135.9, 136.3, 142.1, 144.7, 159.5; MS (ESI): *m/z* [(M + H)<sup>+</sup>]: 434. HRMS *m/z* Calcd for  $C_{20}H_{14}F_3N_3OS_2$  [(M + H)<sup>+</sup>]: 434.1025. Found: 434.1027.

**General procedure.** Ethyl 3-amino-6-(phenyl/thiophen-2-yl)-4-(trifluoromethyl)furo/thieno[2,3-*b*]pyridine-2-carboxylate **3** (0.01 mol) reacted with excess of secondary amines (0.015 mol) and potassium carbonate (0.81 mol) were charged into a round bottom flask, and the mixture was heated at 100°C for 12 h. The reaction mixture was cooled to room temperature, treated with crushed ice, and neutralized with 1-N HCl. The solid precipitate was filtered and washed with excess water, and the crude product was recrystallized from ethanol.

**(3-Amino-6-phenyl-4-(trifluoromethyl)furo[2,3-*b*]pyridin-2-yl)(4-methylpiperazin-1-yl)methanone (5a).** Yellow solid; mp 145–147°C; IR (KBr,  $cm^{-1}$ ): 1668 (–CONH–); <sup>1</sup>H NMR (DMSO-*d*<sub>6</sub>, 300 MHz): δ ppm 2.32 (s, 3H, –CH<sub>3</sub>), 2.84–2.96 (m, 4H, –(CH<sub>2</sub>)<sub>2</sub>–), 3.12–3.25 (m, 4H, –(CH<sub>2</sub>)<sub>2</sub>–), 6.58 (br s, 2H, –NH<sub>2</sub>), 7.38–7.48 (m, 3H, Ar–H), 7.67–7.74 (m, 2H, Ar–H), 8.12 (s, 1H, Py–H); <sup>13</sup>C NMR (DMSO-*d*<sub>6</sub>, 75 MHz): δ ppm 46.3, 49.8, 50.7, 123.7, 125.2, 126.0, 128.0, 129.0, 129.8, 131.3, 133.4, 133.8, 134.6, 142.1, 162.3; MS (ESI): *m/z* [(M + H)<sup>+</sup>]: 434. HRMS *m/z* Calcd for  $C_{20}H_{19}F_3N_4O_2$  [(M + H)<sup>+</sup>]: 405.0126. Found: 405.0128.

**(3-Amino-6-phenyl-4-(trifluoromethyl)thieno[2,3-*b*]pyridin-2-yl)(4-methylpiperazin-1-yl)methanone (5b).** Yellow solid; mp 162–164°C; IR (KBr,  $cm^{-1}$ ): 1665 (–CONH–); <sup>1</sup>H NMR (DMSO-*d*<sub>6</sub>, 300 MHz): δ ppm 2.34 (s, 3H, –CH<sub>3</sub>), 2.79–2.87 (m, 4H, –(CH<sub>2</sub>)<sub>2</sub>–), 3.12–3.23 (m, 4H, –(CH<sub>2</sub>)<sub>2</sub>–), 6.52 (br s, 2H, –NH<sub>2</sub>), 7.36–7.48 (m, 3H, Ar–H), 7.58–7.65 (m, 2H, Ar–H), 8.04 (s, 1H, Py–H); <sup>13</sup>C NMR (DMSO-*d*<sub>6</sub>, 75 MHz): δ ppm 46.0, 49.1, 50.9, 122.8, 123.3, 124.4, 125.4, 126.5, 127.1, 128.0, 129.0, 130.6, 132.2, 136.1, 146.6, 160.8; MS (ESI): *m/z* [(M + H)<sup>+</sup>]: 421. HRMS *m/z* Calcd for  $C_{20}H_{19}F_3N_4OS$  [(M + H)<sup>+</sup>]: 421.0432. Found: 421.0434.

**(3-Amino-6-(thiophen-2-yl)-4-(trifluoromethyl)furo[2,3-*b*]pyridin-2-yl)(4-methylpiperazin-1-yl)methanone (5c).** Yellow solid; mp 152–154°C; IR (KBr,  $cm^{-1}$ ): 1662 (–CONH–); <sup>1</sup>H NMR (DMSO-*d*<sub>6</sub>, 300 MHz): δ ppm 2.61 (s, 3H, –CH<sub>3</sub>), 2.73–2.81 (m, 4H, –(CH<sub>2</sub>)<sub>2</sub>–), 3.75–3.82 (m, 4H, –(CH<sub>2</sub>)<sub>2</sub>–), 6.52 (br s, 2H, –NH<sub>2</sub>), 7.43 (dd, *J* = 4.76, 1H, Ar–H), 7.58 (dd, *J* = 4.72, 1H, Ar–H), 7.83 (s, 1H, Py–H), 8.82 (dd, *J* = 3.72, 1H, Ar–H); <sup>13</sup>C NMR (DMSO-*d*<sub>6</sub>, 75 MHz): δ ppm 46.2, 49.6, 50.9, 120.1,

123.6, 125.5, 126.7, 128.1, 129.0, 130.7, 133.3, 134.3, 135.1, 139.7, 141.9, 159.8; MS (ESI):  $m/z$  [(M + H)<sup>+</sup>]: 411. HRMS  $m/z$  Calcd for C<sub>18</sub>H<sub>17</sub>F<sub>3</sub>N<sub>4</sub>O<sub>2</sub>S [(M + H)<sup>+</sup>]: 411.0251. Found: 411.0254.

**(3-Amino-6-(thiophen-2-yl)-4-(trifluoromethyl)thieno[2,3-b]pyridin-2-yl)(4-methylpiperazin-1-yl)methanone (5d).** Yellow solid; mp 163–164°C; IR (KBr, cm<sup>-1</sup>): 1662 (–CONH–); <sup>1</sup>H NMR (DMSO-*d*<sub>6</sub>, 300 MHz): δ ppm 2.35 (s, 3H, –CH<sub>3</sub>), 2.70–2.82 (m, 4H, –(CH<sub>2</sub>)<sub>2</sub>–), 3.12–3.21 (m, 4H, –(CH<sub>2</sub>)<sub>2</sub>–), 6.51 (br s, 2H, –NH<sub>2</sub>), 7.46 (dd, *J* = 4.72, 1H, Ar–H), 7.54 (dd, *J* = 4.76, 1H, Ar–H), 7.81 (s, 1H, Py–H), 8.82 (dd, *J* = 3.72, 1H, Ar–H); <sup>13</sup>C NMR (DMSO-*d*<sub>6</sub>, 75 MHz): δ ppm 46.2, 49.2, 50.9, 122.0, 125.4, 125.8, 127.0, 128.1, 130.0, 132.0, 134.7, 137.3, 139.9, 142.1, 143.6, 160.5; MS (ESI):  $m/z$  [(M + H)<sup>+</sup>]: 427. HRMS  $m/z$  Calcd for C<sub>18</sub>H<sub>17</sub>F<sub>3</sub>N<sub>4</sub>O<sub>2</sub>S [(M + H)<sup>+</sup>]: 427.0502. Found: 427.0505.

**General procedure.** To the mixture of ethyl 3-amino-6-(phenyl/thiophen-2-yl)-4-(trifluoromethyl)furo/thieno [2,3-*b*]pyridine-2-carboxylate **3** (0.01 mol), L-amino acid (0.02 mol), potassium carbonate (0.05 mol), and dimethyl sulfoxide (10 ml) was added and refluxed for 12 h. The reaction mixture was cooled and diluted with ice water. The aqueous solution was neutralized with 1-N HCl until the pH is neutral. The precipitated solid was filtered, dried, and recrystallized from ethanol.

**2-(3-Amino-6-phenyl-4-(trifluoromethyl)furo[2,3-*b*]pyridine-2-carboxamido)propanoic acid (6a).** Yellow solid; mp 153–155°C; IR (KBr, cm<sup>-1</sup>): 1659 (–CONH–), 1728 (COOH); <sup>1</sup>H NMR (DMSO-*d*<sub>6</sub>, 300 MHz): δ ppm 1.43 (d, 3H, –CH<sub>3</sub>), 4.42–4.51 (m, 1H, –CH–), 6.52 (br s, 2H, –NH<sub>2</sub>), 7.44–7.58 (m, 3H, Ar–H), 7.83 (s, 1H, Py–H), 8.01–8.11 (m, 2H, Ar–H), 8.42 (br s, 1H, –CONH–); <sup>13</sup>C NMR (DMSO-*d*<sub>6</sub>, 75 MHz): δ ppm 16.3, 48.9, 119.5, 120.5, 121.2, 121.8, 123.1, 123.7, 124.6, 125.2, 126.0, 134.6, 142.1, 146.6, 162.8, 170.1; MS (ESI):  $m/z$  [(M + H)<sup>+</sup>]: 394. HRMS  $m/z$  Calcd for C<sub>18</sub>H<sub>14</sub>F<sub>3</sub>N<sub>3</sub>O<sub>4</sub> [(M + H)<sup>+</sup>]: 394.0546. Found: 394.0549.

**2-(3-Amino-6-phenyl-4-(trifluoromethyl)thieno[2,3-*b*]pyridine-2-carboxamido)propanoic acid (6b).** Pale yellow solid; mp 185–187°C; IR (KBr, cm<sup>-1</sup>): 1656 (–CONH–), 1731 (COOH); <sup>1</sup>H NMR (DMSO-*d*<sub>6</sub>, 300 MHz): δ ppm 1.37 (d, 3H, –CH<sub>3</sub>), 4.41–4.52 (m, 1H, –CH–), 6.49 (br s, 2H, –NH<sub>2</sub>), 7.46–7.57 (m, 3H, Ar–H), 7.78 (s, 1H, Py–H), 8.04–8.14 (m, 2H, Ar–H), 8.43 (d, 1H, –CONH–); <sup>13</sup>C NMR (DMSO-*d*<sub>6</sub>, 75 MHz): δ ppm 16.6, 48.9, 121.4, 122.6, 123.5, 125.0, 126.8, 127.1, 129.4, 130.8, 134.9, 136.5, 142.3, 146.4, 160.2, 170.5; MS (ESI):  $m/z$  [(M + H)<sup>+</sup>]: 410. HRMS  $m/z$  Calcd for C<sub>18</sub>H<sub>14</sub>F<sub>3</sub>N<sub>3</sub>O<sub>3</sub>S [(M + H)<sup>+</sup>]: 410.0112. Found: 410.0112.

**2-(3-Amino-6-(thiophen-2-yl)-4-(trifluoromethyl)furo[2,3-*b*]pyridine-2-carboxamido)propanoic acid (6c).** Yellow solid; mp 169–171°C; IR (KBr, cm<sup>-1</sup>): 1658 (–CONH–), 1726 (COOH); <sup>1</sup>H NMR (DMSO-*d*<sub>6</sub>, 300 MHz): δ ppm 1.33

(d, 3H, –CH<sub>3</sub>), 4.32–4.41 (m, 1H, –CH–), 6.51 (br s, 2H, –NH<sub>2</sub>), 7.48 (dd, *J* = 4.71, 1H, Ar–H), 7.78 (dd, *J* = 4.78, 1H, Ar–H), 7.98 (s, 1H, Py–H), 8.09 (dd, *J* = 3.72, 1H, Ar–H), 8.45 (d, 1H, –CONH–); <sup>13</sup>C NMR (DMSO-*d*<sub>6</sub>, 75 MHz): δ ppm 16.6, 48.9, 121.4, 122.6, 123.5, 125.0, 126.8, 127.1, 129.4, 130.8, 134.9, 136.5, 142.3, 146.4, 160.2, 171.3; MS (ESI):  $m/z$  [(M + H)<sup>+</sup>]: 400. HRMS  $m/z$  Calcd for C<sub>16</sub>H<sub>12</sub>F<sub>3</sub>N<sub>3</sub>O<sub>4</sub>S [(M + H)<sup>+</sup>]: 400.0118. Found: 400.0120.

**2-(3-Amino-6-(thiophen-2-yl)-4-(trifluoromethyl)thieno[2,3-*b*]pyridine-2-carboxamido)propanoic acid (6d).** Yellow solid; mp 183–185°C; IR (KBr, cm<sup>-1</sup>): 1660 (–CONH–), 1728 (COOH); <sup>1</sup>H NMR (DMSO-*d*<sub>6</sub>, 300 MHz): δ ppm 1.38 (d, 3H, –CH<sub>3</sub>), 4.26–4.38 (m, 1H, –CH–), 6.52 (br s, 2H, –NH<sub>2</sub>), 7.56 (dd, *J* = 4.74, 1H, Ar–H), 7.79 (dd, *J* = 4.78, 1H, Ar–H), 8.01 (s, 1H, Py–H), 8.15 (dd, *J* = 3.71, 1H, Ar–H), 8.48 (d, 1H, –CONH–); <sup>13</sup>C NMR (DMSO-*d*<sub>6</sub>, 75 MHz): δ ppm 16.8, 47.9, 121.4, 123.7, 124.9, 125.1, 126.4, 128.0, 129.0, 129.9, 131.3, 134.8, 142.2, 146.8, 161.5, 171.3; MS (ESI):  $m/z$  [(M + H)<sup>+</sup>]: 416. HRMS  $m/z$  Calcd for C<sub>16</sub>H<sub>12</sub>F<sub>3</sub>N<sub>3</sub>O<sub>3</sub>S<sub>2</sub> [(M + H)<sup>+</sup>]: 416.1058. Found: 416.1056.

**2-(3-Amino-6-phenyl-4-(trifluoromethyl)furo[2,3-*b*]pyridine-2-carboxamido)-3-phenylpropanoic acid (6e).** Pale yellow solid; mp 199–201°C; IR (KBr, cm<sup>-1</sup>): 1665 (–CONH–), 1725 (COOH); <sup>1</sup>H NMR (DMSO-*d*<sub>6</sub>, 300 MHz): δ ppm 2.69 (d, 2H, –CH<sub>2</sub>–Ph), 4.61–4.72 (m, 1H, –CH–), 6.51 (br s, 2H, –NH<sub>2</sub>), 7.51–7.58 (m, 4H, Ar–H), 7.72–7.85 (m, 6H, Ar–H), 8.15 (s, 1H, Py–H), 8.42 (d, 1H, –CONH–); <sup>13</sup>C NMR (DMSO-*d*<sub>6</sub>, 75 MHz): δ ppm 34.7, 58.0, 120.6, 122.1, 122.8, 124.0, 124.4, 125.6, 125.9, 126.5, 127.2, 128.1, 129.1, 131.5, 132.4, 134.7, 142.0, 146.7, 158.8, 170.6; MS (ESI):  $m/z$  [(M + H)<sup>+</sup>]: 470. HRMS  $m/z$  Calcd for C<sub>24</sub>H<sub>18</sub>F<sub>3</sub>N<sub>3</sub>O<sub>4</sub> [(M + H)<sup>+</sup>]: 470.0189. Found: 470.0191.

**2-(3-Amino-6-phenyl-4-(trifluoromethyl)thieno[2,3-*b*]pyridine-2-carboxamido)-3-phenylpropanoic acid (6f).** Pale yellow solid; mp 182–184°C; IR (KBr, cm<sup>-1</sup>): 1660 (–CONH–), 1731 (COOH); <sup>1</sup>H NMR (DMSO-*d*<sub>6</sub>, 300 MHz): δ ppm 2.71 (d, 2H, –CH<sub>2</sub>–Ph), 4.42–4.51 (m, 1H, –CH–), 6.52 (br s, 2H, –NH<sub>2</sub>), 7.42–7.56 (m, 4H, Ar–H), 7.72–7.87 (m, 6H, Ar–H), 8.03 (s, 1H, Py–H), 8.41 (d, 1H, –CONH–); <sup>13</sup>C NMR (DMSO-*d*<sub>6</sub>, 75 MHz): δ ppm 34.7, 58.0, 121.0, 122.7, 123.4, 124.6, 125.0, 125.9, 126.7, 127.8, 128.6, 129.0, 129.4, 131.3, 132.4, 134.7, 143.0, 147.3, 159.9, 171.3; MS (ESI):  $m/z$  [(M + H)<sup>+</sup>]: 486. HRMS  $m/z$  Calcd for C<sub>24</sub>H<sub>18</sub>F<sub>3</sub>N<sub>3</sub>O<sub>3</sub>S [(M + H)<sup>+</sup>]: 486.0287. Found: 486.0287.

**2-(3-Amino-6-(thiophen-2-yl)-4-(trifluoromethyl)furo[2,3-*b*]pyridine-2-carboxamido)-3-phenylpropanoic acid (6g).** Yellow solid; mp 196–198°C; IR (KBr, cm<sup>-1</sup>): 1662 (–CONH–), 1734 (COOH); <sup>1</sup>H NMR (DMSO-*d*<sub>6</sub>, 300 MHz): δ ppm 2.72 (d, 2H, –CH<sub>2</sub>–Ph), 4.42–4.51 (m, 1H, –CH–), 6.50 (br s, 2H, –NH<sub>2</sub>), 7.42 (dd, *J* = 4.74,

<sup>1</sup>H, Ar-H), 7.48–7.53 (m, 3H, Ar-H), 7.65–7.68 (m, 2H, Ar-H), 7.73 (dd, *J* = 3.72, 1H, Ar-H), 7.81 (dd, *J* = 4.74, 1H, Ar-H), 8.11 (s, 1H, Py-H), 8.43 (d, 1H, –CONH–); <sup>13</sup>C NMR (DMSO-*d*<sub>6</sub>, 75 MHz): δ ppm 34.0, 57.2, 120.3, 121.8, 122.5, 123.7, 124.0, 125.0, 125.9, 126.8, 127.7, 128.0, 128.8, 131.3, 132.5, 134.7, 143.0, 147.7, 160.0, 170.9; MS (ESI): *m/z* [(M + H)<sup>+</sup>]: 476. HRMS *m/z* Calcd for C<sub>22</sub>H<sub>16</sub>F<sub>3</sub>N<sub>3</sub>O<sub>4</sub>S [(M + H)<sup>+</sup>]: 476.0615. Found: 476.0618.

**2-(3-Amino-6-(thiophen-2-yl)-4-(trifluoromethyl)thieno[2,3-*b*]pyridine-2-carboxamido)-3-phenylpropanoic acid (6h).** Yellow solid; mp 181–183°C; IR (KBr, cm<sup>-1</sup>): 1665 (–CONH–), 1737 (COOH); <sup>1</sup>H NMR (DMSO-*d*<sub>6</sub>, 300 MHz): δ ppm 2.64 (d, 2H, –CH<sub>2</sub>–Ph), 4.42–4.52 (m, 1H, –CH–), 6.54 (br s, 2H, –NH<sub>2</sub>), 7.44 (dd, *J* = 4.72, 1H, Ar-H), 7.48–7.52 (m, 3H, Ar-H), 7.58–7.64 (m, 2H, Ar-H), 7.78 (dd, *J* = 4.74, 1H, Ar-H), 7.84 (dd, *J* = 3.71, 1H, Ar-H), 8.23 (s, 1H, Py-H), 8.42 (d, 1H, –CONH–); <sup>13</sup>C NMR (DMSO-*d*<sub>6</sub>, 75 MHz): δ ppm 34.4, 58.2, 120.6, 122.1, 122.7, 123.8, 124.3, 125.2, 125.8, 126.9, 128.4, 129.0, 129.3, 132.0, 133.0, 134.7, 143.0, 147.6, 159.4, 171.5; MS (ESI): *m/z* [(M + H)<sup>+</sup>]: 492. HRMS *m/z* Calcd for C<sub>22</sub>H<sub>16</sub>F<sub>3</sub>N<sub>3</sub>O<sub>3</sub>S<sub>2</sub> [(M + H)<sup>+</sup>]: 492.0118. Found: 492.0115.

## CONCLUSION

In conclusion, a series of novel alkyl amide functionalized trifluoromethyl substituted furo/thieno pyridine derivatives **4a–h**, **5a–d**, and **6a–h** were prepared and evaluated for anticancer against four human cancer cell lines. Among all the compounds screened, the compounds **4g** and **4h** showed significant activity against all cell lines at micromolar concentration (8.5–16.8 μM). 3D-QSAR, CoMFA, and CoMSIA studies have been applied to alkyl amide functionalized trifluoromethyl substituted furo/thieno pyridine derivatives. Both these CoMFA and CoMSIA models for HeLa and COLO205 inhibitors generated have confirmed to be statistically precise with higher *q*<sup>2</sup> and *r*<sup>2</sup>. The information achieved from CoMFA and CoMSIA models could lead to a better design of novel selective and higher potent alkyl amide functionalized trifluoromethyl substituted furo/thieno pyridine derivatives as anticancer agents.

**Acknowledgments.** Author Srinu Bhoomandla is thankful to the Director, Gitam University, Hyderabad, for providing lab facility and Malla Reddy Institute of Technology and Science, Secunderabad, for constant encouragement.

## REFERENCES AND NOTES

[1] Anand, P.; Kunnumakara, A. B.; Sundaram, C.; Harikumar, K. B.; Tharakan, S. T.; Lai, O. S.; Sung, B.; Aggarwal, B. B. *Pharm Res* 2008, 25, 2097.

- [2] Baraldi, P. G.; Cacciari, B.; Romagnoli, R.; Spalluto, G.; Monopoli, A.; Ongini, E.; Varani, K.; Borea, P. A. *J Med Chem* 2002, 45, 115.
- [3] Goodacre, S. C.; Street, L. J.; Hallett, D. J.; Crawforth, J. M.; Kelly, S.; Owens, A. P.; Blackaby, W. P.; Lewis, R. T.; Stanley, J.; Smith, A. J.; Ferris, P.; Sohal, B.; Cook, S. M.; Pike, A.; Brown, N.; Wafford, K. A.; Marshall, G.; Castro, J. L.; Atack, J. R. *J Med Chem* 2006, 49, 35.
- [4] Chen, C.; Wilcoxon, K. M.; Huang, C. Q.; Xie, Y. F.; McCarthy, J. R.; Webb, T. R.; Zhu, Y. F.; Saunders, J.; Liu, X. J.; Chen, T. K.; Bozigan, H.; Grigoriadis, D. E. *J Med Chem* 2004, 47, 4787.
- [5] (a) Dai, H.; Yu, H. B.; Liu, J. B.; Li, Y. Q.; Qin, X.; Zhang, X.; Qin, Z. F.; Wang, T. T.; Fang, J. *ARKIVOC* 2009, 7, 126; (b) Duan, M.; Kazmierski, W. M.; Chong, P. Y.; De Anda, F.; Edelstein, M.; Ferris, R.; Peckham, J.; Wheelan, P.; Xiong, Z.; Zhang, H.; Nishizawa, R.; Takaoka, Y. *Bioorg Med Chem Lett* 2011, 21, 6470.
- [6] Luedtke, G. R.; Schinzel, K.; Tan, X.; Tester, R. W.; Nashashibi, I.; Xu, Y.; Dugar, S.; Levy, D. E.; Jung, J. *Bioorg Med Chem Lett* 2010, 20, 2556.
- [7] (a) Packiarajan, M.; Coate, H.; Desai, M.; Jimenez, H. N.; Reinhard, E. J.; Jubian, V. J.; Marzabadi, M. R.; Chandrasena, G.; Wolinski, T. C.; Walker, M. W.; Andersen, K. *Bioorg Med Chem Lett* 2011, 21, 6500; (b) Dewang, P. M.; Dae-Kee, K. *Bioorg Med Chem Lett* 2010, 20, 4228.
- [8] Ge, J. F.; Arai, C.; Yang, M.; Bakar, M.; Lu, J.; Ismail, N. S. M.; Wittlin, S.; Kaiser, M.; Brun, R.; Charman, S. A.; Nguyen, T.; Morizzi, J.; Itoh, I.; Ihara, M. *ACS Med Chem Lett* 2010, 1, 360.
- [9] Kawakami, K.; Takahashi, H.; Ohki, H.; Kimura, K.; Miyauchi, S.; Miyauchi, R.; Takemura, M. *Chem Pharm Bull* 2000, 48, 1667.
- [10] Ledoossal, B.; Boazard, D.; Coroneos, E. *J Med Chem* 1992, 35, 198.
- [11] Dorsey, B. D.; McDonough, C.; McDaniel, S. L.; Levin, R. B.; Newton, C. L.; Hoffman, J. M.; Darke, P. L.; Zugay-Murphy, J. A.; Emimi, E. A.; Schlieff, W. A.; Olsen, D. B.; Stahlhut, M. W.; Rutkowski, C. A.; Kuo, L. C.; Lin, J. H.; Chen, I.-W.; Michelson, S. R.; Holloway, M. K.; Huff, J. R.; Vacca, J. P. *J Med Chem* 2000, 43, 3386.
- [12] Bhupathy, M.; Conlon, D. A.; Wells, K. M.; Nelson, J. R.; Reider, P. J.; Rossen, K.; Sager, J. W.; Volante, R. P.; Dorsey, B. D.; Hoffman, J. M.; Joseph, S. A.; McDaniel, S. L. *J Heterocyclic Chem* 1995, 32, 1283.
- [13] (a) Choi, W.-B.; Houppis, I. N.; Churchill, H. R. O.; Molina, A.; Lynch, J. E.; Volante, R. P.; Reider, P. J.; King, A. O. *Tetrahedron Lett* 1995, 36, 4571; (b) Houppis, I. N.; Choi, W.-B.; Reider, P. J.; Molina, A.; Churchill, H.; Lynch, J.; Volante, R. P. *Tetrahedron* 1994, 35, 9355.
- [14] (a) Yonishi, S.; Itani, H.; Sato, Y.; Tsutsumi, H.; Akahane, A. *PCT Int. Appl.*, WO 2004089939 A1, 2004; (b) Toupenche, R. B.; Debenham, J. S.; Goulet, M. T.; Madsen-Duggan, C. B.; Walsh, T. F.; Shah, S. K. *PCT Int Appl*, WO 2004012671 A2, 2004.
- [15] VanSickle, A. P.; Rapoport, H. *J Org Chem* 1990, 55, 895.
- [16] Malamas, M. S.; Sredy, J.; Moxham, C.; Katz, A.; Xu, W.; McDevitt, R.; Adebayo, F. O.; Sawicki, D. R.; Seestaller, L.; Sullivan, D.; Taylor, J. R. *J Med Chem* 2000, 43, 1293.
- [17] Nair, V. A.; Mustafa, S. M.; Mohler, M. L.; Fisher, S. J.; Dalton, J. T.; Miller, D. D. *Tetrahedron Lett* 2004, 45, 9475.
- [18] Ohtsu, H.; Xiao, Z.; Ishida, J.; Nagai, M.; Wang, H. K.; Itokawa, H.; Su, C. Y.; Shih, C.; Chiand, T.; Chang, E.; Lee, Y.; Tsai, M. Y.; Chang, C.; Lee, K. H. *J Med Chem* 2002, 45, 5037.
- [19] Kurumurthy, C.; Sambasiva Rao, P.; Veeraswamy, B.; Santhosh Kumar, G.; Shanthan Rao, P.; Narsaiah, B.; Velatooru, L. R.; Pamanji, R.; Venkateswara, R. J. *Eur J Med Chem* 2011, 46, 3462.
- [20] Sirisha, B.; Narsaiah, B.; Yakaiah, T.; Gayatri, G.; Sastry, G. N.; Prasad, M. R.; Rao, A. R. *Eur J Med Chem* 2010, 45, 1739.
- [21] Santhosh Kumar, G.; Poornachandra, Y.; Ratnakar Reddy, K.; Ganesh Kumar, C.; Narsaiah, B. *Syn Comm* 2017, 47, 1864.
- [22] Mosmann, T. *J Immunol Methods* 1983, 65, 55.
- [23] Gunda, S. K.; Kongaleti, S. F.; Shaik, M. *Int J Comput Biol Drug Des* 2015, 8, 19.
- [24] Pan, Y.; Li, P.; Xie, S.; Tao, Y.; Chen, D.; Dai, M.; Hao, H.; Huang, L.; Wang, Y.; Wang, L.; Liu, Z.; Yuan, Z. *Bioorg Med Chem Lett* 2016, 26, 4146.

- [25] Klebe, G.; Abraham, U.; Mietzner, T. *J Med Chem* 1994, 37, 4130.
- [26] Clark, M. *Comput Chem* 1989, 10, 982.
- [27] Hu, R.; Barbault, F.; Delamar, M.; Zhang, R. *Bioorg Med Chem* 2009, 17, 2400.
- [28] AbdulHameed, M. D.; Hamza, A.; Liu, J.; Zhan, C. G. *J Chem Inf Model* 2008, 48, 1760.
- [29] Cho, S. J.; Tropsha, A. *J Med Chem* 1995, 38, 1060.

## SUPPORTING INFORMATION

Additional supporting information may be found online in the Supporting Information section at the end of the article.